energy&fuels

Article

pubs.acs.org/EF

Asphaltenes Transport into Catalysts under Hydroprocessing Conditions

Florine Gaulier,[†] Jérémie Barbier,[†] Bertrand Guichard,[†] Pierre Levitz,[‡] and Didier Espinat*[,†]

[†]IFP Energies nouvelles, Rond-point de l'échangeur de Solaize, BP 3, 69360 Solaize, France

[‡]Laboratoire PHENIX, Université Pierre et Marie Curie, 4 place Jussieu, 72522 Paris Cedex 5, France

ABSTRACT: Heavy oil fractions can be upgraded through various processes, such as catalytic residue hydrotreatments. Mass transfer of macromolecules present in the heavy oil fraction, so-called asphaltenes, from feedstock to catalytic active sites is limited during hydroprocesses. Mechanisms of the diffusion of asphaltenes through pore network, adsorption, and pore plugging are no well-known under process conditions. A new method has been developed to characterize and investigate asphaltene diffusion phenomenon in catalysts under a high temperature and pressure. Alumina supports immersed in asphaltene solution are left to evolve at 250 °C and 5.0 MPa. Solutions and supports are analyzed to quantify the mass transfer, penetration depth, and change in support porosity of asphaltenes. This procedure was evaluated in terms of reproducibility and sensitivity. The impact of several parameters, such as pressure, was appraised. With this powerful procedure, for the first time, asphaltene diffusion without conversion into the pore network of a catalyst at a high temperature and pressure has been monitored over time. In accordance with analytical results, we proposed a primary model for the asphaltene adsorption and pore network cluttering mechanism under hydroprocessing conditions.

1. INTRODUCTION

Because sources of conventional crude oils decrease, the deep conversion of a residue increases to produce gasoline and middle distillate, whose demand is strongly increasing. The main characteristic of residues is the presence of asphaltenes, which constitute the most polar fraction of these products.

Asphaltenes are responsible for diffusion limitations. The flocculation of asphaltenes induces pore plugging and permeability reduction during reservoir exploitation.[1,2] In deep conversion processes, asphaltene macromolecules have an important effect on the catalytic process efficiency and catalyst life cycle.[3]

Asphaltenes are polyaromatic hydrocarbons. They constitute a complex mixture of molecules in terms of size and chemical composition, which depend upon various factors, such as their geological sources and extraction methods.[4] These molecules have demonstrated self-assembling capacities, forming aggregates in a large range of sizes. This aggregation is dependent upon the type of solvent, concentration, and temperature.[5−8] Two types of aggregates are measured at ambient conditions in the residue, in agreement with the Yen−Mullins model of asphaltene aggregation.[9] For example, small-angle X-ray scattering (SAXS) measurements have highlighted the disaggregation phenomenon with the increase of the temperature from 80 to 200 °C, noticing a drop of the average radius of gyration of asphaltene aggregates in a vacuum residue from 40.4 to 32.6 Å.[7]

Brownian motion of asphaltenes has been studied by different analytical tools, such as fluorescence correlation spectroscopy and dynamic light scattering.[10,11] However, these techniques measured a global diffusion coefficient, where asphaltene is a mixture of polydisperse aggregates. Nuclear magnetic resonance (NMR) with diffusion-ordered spectroscopy (DOSY) experiments have measured self-diffusion coefficients and can distinguish multiple asphaltene aggregates in a model solvent.[12] In toluene, the diffusion coefficient of asphaltenes was measured from DOSY NMR experiments in a large range of self-diffusion coefficients in order of magnitude of 1×10^{-10} m^2/s, depending upon their geological sources and their concentrations in solution.[13]

The transport through catalyst porosity is less known. Studies with *in situ* measurements have monitored mass transfer at ambient conditions in porous media.[14−16] The concentration in the liquid phase over time is recorded with *in situ* measurements by ultraviolet−visible spectrometry,[17] and *ex situ* analyses were also explored to determine the change in accessibility in the support.[18] This kind of experiment was coupled with mathematical modeling. The most used models assumed a single type of asphaltene pore cluttering process based on Langmuir adsorption and has shown an effective diffusion coefficient of asphaltenes in toluene into catalyst in order of magnitude of 1×10^{-12} m^2/s.[17]

At a high temperature and pressure, studies on the hydroconversion process give clues in diffusion limitation of asphaltenes in catalysts.[19,20] The characterization by size-exclusion chromatography of effluents showed a limitation in conversion of the largest asphaltenes. For example, the size of the asphaltenes containing metal significantly impacts their reactivity during hydrotreatment. At a high molecular weight, asphaltenes above 5 kDa are the most refractory to conversion.[21] Some studies characterize also the metal content deposition in porous media and porosity alteration.[22] However, to our knowledge, no measurement of asphaltene transport into

Received: June 22, 2015
Revised: August 17, 2015
Published: September 2, 2015

DOI: 10.1021/acs.energyfuels.5b01355
Energy Fuels 2015, 29, 6250−6258

porous media without conversion was monitored under a high temperature and pressure.

This paper proposed a new method developed to characterize and investigate the asphaltene transport phenomenon in catalysts under hydroprocessing conditions. Alumina supports immersed in asphaltene solution are left to evolve at a high temperature and pressure. *Ex situ*, solutions and supports are analyzed to quantify the mass transfer, penetration depth, and change in support porosity of asphaltenes. Reproducibility of the procedure was evaluated. Influences of stirring, imbibition, and pressure were studied. To investigate the asphaltene deposition phenomenon, the mass transfer was compared to porosity characterization and asphaltene penetration depth, which gave substantial clues on the asphaltene pore cluttering mechanism.

2. EXPERIMENTAL SECTION

2.1. Analytes. *2.1.1. Solutions.* Solutions of asphaltenes in toluene were used to observe specifically asphaltene diffusion. Asphaltenes have been extracted by *n*-heptane precipitation from a Safaniya vacuum residue according to the NF T60-115 method. Asphaltene characteristics were summarized in Table 1. Asphaltene solutions were prepared by dissolution in toluene at required concentrations, ranging from 1 to 3 wt %. Toluene and *n*-heptane were purchased from Aldrich with 99.5 and 99% grade, respectively.

Table 1. Characteristics of Asphaltenes

H/C ratio	1.10 ± 0.05
S content (wt %)	8 ± 2
vanadium content (ppm)	550 ± 50
nickel content (ppm)	190 ± 30
structural density, ρ_{struc} (g/mL)	1.22 ± 0.06

2.1.2. Porous Media. In the purpose of avoiding asphaltene conversion during the procedure, it was chosen to use an alumina support without metallic active sites. A standard γ-Al_2O_3 hydrotreating catalyst support was considered as representative of the porous media.

Alumina supports were cylindrical extrudates with 3 mm diameter and an average 10 mm length. They had a meso single-mode pore size distribution. The supports were calcined and treated under hot vapor to reach the main characteristics summarized in Table 2. They were dried for at least 6 h at 150 °C prior to being used.

Table 2. Characteristics of Alumina Supports

specific surface area, S_{BET} (m^2/g)	194 ± 10
parameter *C* from the BET	113 ± 6
porous volume, V_{BJH} (mL/g)	0.80 ± 0.04
mean pore diameter, d_{mean} (nm)	14.5 ± 0.7
structural density, ρ_{struc} (g/mL)	3.22 ± 0.32
porosity, ε (%)	71 ± 4

2.2. Equipment. A high pressure and temperature unit detailed in Figure 1 was set up. It is made of a hermetic cell of an internal volume of 50 mL, an electrical heater, and a control panel. This unit was equipped with internal temperature and pressure sensors. The temperatures of the external surface of the cell and the resistor of the electrical heater were also monitored. The cell was connected to dry N_2 gas. Solution homogeneity was ensured by a magnetic stirrer. A basket was designed to protect the alumina supports against magnetic stir damages.

2.3. Analysis. *2.3.1. Optical Microscopy.* The penetration depth of the asphaltenes was followed by an optical microscopy method developed in our previous work.[15] Extrudates were cut in half and coated in TransOptic thermoplastic acrylic resin at 180 °C and 15 kN.

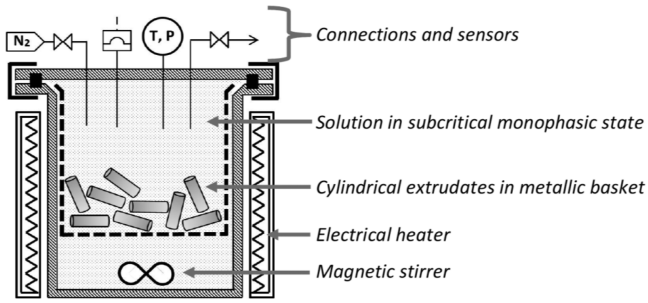

Figure 1. High temperature and pressure unit.

Then, they were polished with abrasive paper SiC 2500. Observations were made through an Olympus BX51 microscope in reflection mode completed with a polarizer filter. Images were taken with a charge-coupled device (CCD) color camera and 2.5× zoom at a resolution of 2080 × 1544, allowing for a sensitivity of 2.7 μm/pixel.

2.3.2. Porosity Characterization. Porosity characteristics of the supports were determined by nitrogen adsorption and mercury porosimetry techniques according to ASTM D3663-03 and ASTM D4284-03 methods, respectively. Samples were pretreated for 6 h at 150 °C and then placed into a desiccator for 30 min before analyses.

The nitrogen adsorption procedure used a Micromeritics ASAP 2420 analyzer. This analysis is used to measure the specific surface area (S_{BET}) in m^2/g with the Brunauer–Emmett–Teller (BET) method.[23] In this method, the parameter *C* might be used to appraise the nitrogen affinity to the support surface.[24]

For mesopores, size distribution determination is usually applied with the consideration of the desorption branch of the nitrogen isotherm,[25] specifically in our case with a nitrogen isotherm of type IVa.[24] The pore volume (V_{BJH}) is measured in mL/g between 4 and 80 nm of pore diameter (d_{pores}) by nitrogen desorption with the Barrett–Joyner–Halenda (BJH) method.[26] The pore diameter distribution has been appraised by plotting pore size versus pore volume deviation ($\partial V_{BJH}/\partial d_{pores}$). The mean pore diameter (d_{mean}) in nanometers was measured as the pore diameter at the maximum of porous volume deviation.

The mercury porosimetry procedure used a Micromeritics AutoPore IV 9500 analyzer. This technique allows for measurements of the internal porosity (ε) of extrudates in percent and structural density (ρ_{str}) in g/mL.

2.4. Procedure. *2.4.1. Temperature and Pressure Profile.* With the unit volume constant, pressure varies with the amount of solution and the temperature. Experiments were carried out at 250 °C to avoid thermal cracking of asphaltenes.[27] To avoid a triphasic system with a gas-phase equilibrium, the pressure was set to induce a subcritical liquid monophasic state of the toluene solution. The working pressure was set between 1.8 and 9.0 MPa. The pressure was adjustable within 1.0 MPa. A variation of 0.2 g on solution mass induced a variation of 0.7 MPa on final pressure, while the final pressure depends upon the temperature with a sensitivity of about 0.3 MPa/°C.

As depicted in Figure 2, during the heating step, the unit reached 238 °C after 27 min of heating. During this step, the pressure increase followed vapor saturation pressure of toluene, and beyond 238 °C, the pressure dramatically increased, showing that solution is becoming a subcritical state. The pressure is then stabilizing in approximately 20 min.

The residence time (t_R) was defined as the period between when 95% of the set temperature is achieved and when cooling is started. Residence times were set in a range from a few hours to 3 weeks.

The aim of the cooling step is to stop the diffusion process. The cell is taken off from the heater and became cold with external air flow until the temperature reached 40 °C. This step takes 16 min. At 40 °C, the vent is open to release extra pressure.

On the basis of time for heating and cooling steps, the transition periods may be neglected to the studied residence time of several days. Besides, an experiment with no residence time was performed to

DOI: 10.1021/acs.energyfuels.5b01355
Energy Fuels 2015, 29, 6250–6258

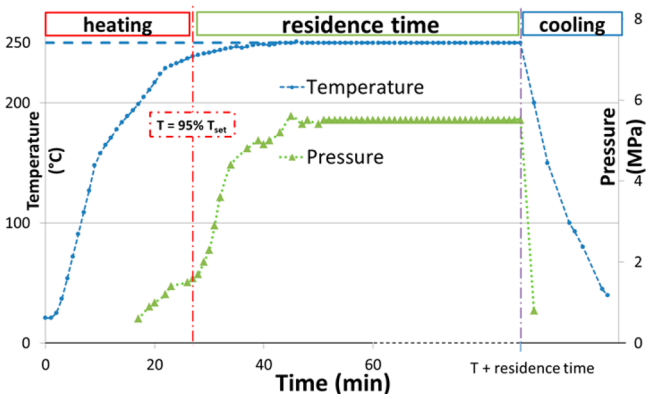

Figure 2. Temperature and pressure recorded during an experiment at 250 ± 1 °C and 5 ± 1 MPa.

investigate the influence of these steps on the diffusion process of a few hours.

2.4.2. Load and Unload of the Unit. To avoid under- or oversaturation of the surface of alumina, the isotherm of adsorption at ambient temperature of a previous study[17] was taken into account to choose a set ratio of asphaltenes introduced to alumina of 360 mg/g. A mass of 2 g of extrudates was selected to have representative numbers of extrudates (approximately 60 extrudates). The volume of solution was set in accordance with the target temperature and pressure equilibrium required. The initial concentration of the asphaltene solution is deducted from this volume.

The supports were immersed in solution prior to sealing and weighing the whole unit. The air of the headspace was purged briefly with dry nitrogen gas. Afterward, the unit was weighed to detect any significant loss during the experiment. Solutions were magnetically stirred at 1400 rpm and then heated.

After unit cycle, supernatants were separated from supports by filtration on 0.45 μm filter paper. Wet supports were briefly washed with cold toluene and dried at 150 °C in a heating chamber for at least 6 h. The unit was also washed with toluene to avoid any asphaltene loss. The analyses were carried out *ex situ* on solutions and supports.

2.4.3. Mass Balance. A mass balance on asphaltenes was performed for each experiment. This calculation was made according to eq 1

$$\mathrm{MB} = \frac{C_f m_f + \Delta m_s + C_r m_r}{C_i m_i} \quad (1)$$

with MB being the mass balance, Δm_s being the difference between the initial dry support mass and impregnated support mass after toluene evaporation, and $C_i m_i$, $C_f m_f$, and $C_r m_r$ being asphaltene concentrations multiplied by masses for initial solution (i), supernatant after experiment (f), and toluene used to wash the unit and supports (r), respectively.

To calculate MB, variation of support mass during experiment (Δm_s) was assumed to be due to only asphaltene penetration. Thus, water and toluene evaporations were supposed to be complete after drying steps.

The concentrations of supernatant and washed toluene were evaluated by weighing the residue after solvent evaporation. About 10 g aliquots were weighed in a glass dish. Because of its highly volatility, toluene was evaporated at ambient temperature under air vacuum at 400 N m^3 h^{-1}. The remaining residue was finally dried at 60 °C in a heating chamber for at least 2 h.

The concentration of asphaltenes in supports could be calculated from asphaltene loss in solutions following eq 2 or from the increase of support mass eq 3

$$q_{\mathrm{asph}} = \frac{C_i m_i - C_f m_f - C_r m_r}{m_s} \quad (2)$$

$$q_{\mathrm{asph}} = \frac{\Delta m_s}{m_s} \quad (3)$$

with q_{asph} being the asphaltene concentration in supports, expressed in milligrams of asphaltenes per gram of alumina and m_s being the initial mass of the support.

2.4.4. Method Evaluation. 2.4.4.1. Limits of Detection and Quantification in Mass Balance. The limits of quantification and detection of Δm_s and concentrations of solutions (C_f and C_r) were experimentally measured following the NF T90-210 method.

For support mass variation, 2 g of dry supports was imbibed with toluene for 5 days at ambient temperature. They were then dried, and mass variations were recorded. The detection and quantification limits were evaluated for five measurements with the following equations:

$$\mathrm{LD} = \bar{x}_0 + 3s_0 \quad (4)$$

$$\mathrm{LQ} = \bar{x}_0 + 10s_0 \quad (5)$$

with LD and LQ being the detection and quantification limits, respectively, and $\bar{x}_0$ and s_0 being the average response and standard deviation of blank measurements, respectively.

For solution concentration, the measurements were carried out with toluene, which has been put in contact with supports for 5 days at ambient temperature. Toluene was separated from supports following the procedure. Then, concentrations in toluene were evaluated with 10 g of aliquot. In analogy with support mass variation, the detection and quantification limits were evaluated with five measurements according to eqs 4 and 5.

The detection and quantification limits of support mass variation, Δm_s, were evaluated at 6 and 20 mg, respectively. For solution concentrations (C_f and C_r), the detection and quantification limits were evaluated at 0.01 and 0.04 wt %. Considering a supernatant mass at 35 g, it can be extrapolated that the limit of quantification of asphaltenes in this solution is 14 mg in the supernatant and the detection limit is 4 mg.

2.4.4.2. Blank Testing. Different types of blank test were performed to evaluate errors induced by the use of the unit. The experiments were performed in the unit with a t_R of 3 h, at 250 °C and about 5.0 MPa.

Blank tests called A were performed in duplicate with toluene in contact with alumina supports. Blank tests called B were carried out in duplicate with solution at 2 wt % without porous media. Following each B blank test, the washing efficiency was assessed to quantify a possible impact of residual asphaltenes on the following experiment. To do so, an additional test called C were carried out with only toluene. The results of the blank testing were summarized in Table 3.

In the case of A blank tests, all measurements were below the asphaltene limit of detection. Thus, a significant pollution from manipulation or equipment was not detected, which could have a decrease in procedure sensitivity.

Table 3. Blank Testing of the Procedure and Washing Efficiency Assessment

	A (without asphaltenes)	B (without support)	C (additional washing)
initial mass of asphaltenes, $C_i m_i$ (mg)	0	724	0
mass of asphaltenes in support, Δm_s (mg)	3 (<LD)	n/a	n/a
concentration of asphaltenes in supernatant, C_f (wt %)	0.00 (<LD)	1.98	0.00 (<LD)
concentration of asphaltenes in washed toluene, C_r (wt %)	0.00 (<LD)	0.01 (<LQ)	0.00 (<LD)
mass balance, MB (%)	n/a	98	n/a

DOI: 10.1021/acs.energyfuels.5b01355
Energy Fuels 2015, 29, 6250−6258

Table 4. Mass Balance of Reliability Tests

	without stirring	pre-imbibition	at 18 bar	at 90 bar
conditions of T, P, and t_R	250 °C, 50 bar, and 3 h	250 °C, 58 bar, and 3 h	250 °C, 18 bar, and 3 h	250 °C, 90 bar, and 3 h
ratio of asphaltenes/support (mg/g)	359 ± 1	353 ± 1	358 ± 1	360 ± 1
initial mass of asphaltenes, $C_i m_i$ (mg)	721 ± 2	716 ± 2	705 ± 2	720 ± 2
mass of asphaltenes in the support, Δm_s (mg)	147 ± 2	149 ± 2	159 ± 2	144 ± 2
mass of asphaltenes in the supernatant, $C_f m_f$ (mg)	554 ± 2	518 ± 2	521 ± 2	542 ± 2
mass of asphaltenes in washed toluene, $C_r m_r$ (mg)	19 < LQ	18 < LQ	15 < LQ	16 < LQ
mass balance, MB (%)[a]	100 ± 1	96 ± 1	99 ± 1	97 ± 1
asphaltene concentration in supports, q_{asp} (mg/g)[b]	74 ± 10	89 ± 12	86 ± 12	81 ± 11

[a]Taking into account of the asphaltene mass in washed toluene. [b]Concentration with the remainder method (eq 2) and ± with the 14% relative repeatability of the procedure (cf. to section 3.2).

Table 5. Mass Balance of Asphaltene Diffusion Experiments with Different Residence Times

	0 min	90 min	3 h	1 day	5 days	3 weeks
conditions of T, P, and t_R	238 °C, 17 bar, and 0 min	250 °C, 41 bar, and 90 min	250 °C, 50 bar, and 3 h	250 °C, 39 bar, and 24 h	250 °C, 39 bar, and 5 days	250 °C, 40 bar, and 22 days
ratio of asphaltenes/support (mg/g)	357 ± 1	358 ± 1	362 ± 1	361 ± 1	360 ± 1	358 ± 1
initial mass of asphaltenes, $C_i m_i$ (mg)	724 ± 1	724 ± 1	727 ± 1	722 ± 1	723 ± 1	722 ± 1
mass of asphaltenes in the support, Δm_s (mg)	60 ± 2	121 ± 2	136 ± 2	243 ± 2	313 ± 2	396 ± 2
mass of asphaltenes in the supernatant, $C_f m_f$ (mg)	664 ± 8	585 ± 8	557 ± 8	462 ± 9	395 ± 7	311 ± 2
mass of asphaltenes in washed toluene, $C_r m_r$ (mg)	<LD[a]	<LD[a]	<LD[a]	<LD[a]	<LD[a]	<LD[a]
mass balance, MB (%)	100 ± 1	98 ± 1	95 ± 1	98 ± 2	98 ± 1	99± 1
asphaltene concentration in supports, q_{asp} (mg/g)[b]	29 ± 4	69 ± 4	84 ± 4	130 ± 5	163 ± 4	204 ± 2

[a]LD = limit of detection; 5 mg of asphaltenes in solution (cf. to section 3.1). [b]Concentration with the remainder method (eq 2) and ± with the measurement error.

In B blank test, 98% of initial introduced asphaltenes was found back after tests. It can be noticed that washed toluene contained asphaltenes but under the quantification limit. We considered that equipment and procedure manipulation did not induce a significant loss of asphaltenes in our conditions.

The results of C tests were all below the limit of detection. It indicates that no significant amount of asphaltenes was trapped in the tubing of the unit or reversibly adsorbed on the cell surface after experiments. Thus, it can be concluded that there is no experiment-to-experiment pollution with our toluene wash procedure.

2.4.4.3. Repeatability Tests. Repeatability tests were performed following the procedure with the contact of the solution and supports of asphaltenes, at 250 °C, approximately 5.0 MPa, and a t_R of 3 h. The experiment was carried out 5 times at different dates with different batches of solutions and supports.

In our experiments, mass losses, recorded with unit weighing, did not exceed 0.2 g, which is lower than 1% of total solution mass. These mass losses were attributed to unit manipulation and were not taken into account in mass balances of asphaltenes.

The ratio of asphaltenes to support was adjusted to 361 ± 1 mg/g. From 723 ± 3 mg of initial asphaltenes introduced, it was found back 555 ± 25 mg in solution and 150 ± 25 mg on supports. The whole procedure exhibits an average asphaltene mass balance of 98 ± 5 %. The average asphaltene concentration in supports calculated according to eq 2 was 83 ± 12 mg/g. Thus, this repeatability of 14% relative error on asphaltenes in an alumina concentration measurement was applied on subsequent measurements to assess the relevance of the results.

2.4.4.4. Influence of the Parameters of the Procedure. Different experiments were carried out to measure the influence of various procedure parameters in the diffusion measurement at 250 °C and with a t_R of 3 h.

An experiment without stirring was carried out and compared to the experience with stirring at 1400 rpm to appraise the influence of external transport limitations in our measurement.

In first time of asphaltene diffusion, as a result of toluene quick penetration into the support, some asphaltenes might be brought straight to the center of the support. To limit this imbibition effect, a pre-imbibition of the support with toluene might be necessary. Thus, an experiment with a pre-imbibition step was carried out and compared to our procedure, to assess its impact. Dry supports were imbibed with toluene and stabilized for 3 h prior to being used following the procedure.

The unit allows for a pressure setting accuracy of 1.0 MPa. To study the effect of the pressure, two experiments were performed at 1.8 and 9.0 MPa, respectively.

3. RESULTS AND DISCUSSION

3.1. Influence of the Parameters of the Procedure.

The results of the parameters of the procedure tests were summarized in Table 4.

In the experiment without stirring, the asphaltene concentration in supports was recorded at 74 ± 10 mg/g, which is lower than the experiment with stirring, but this result remains inside the procedure repeatability error previously mentioned. Thus, stirring does not significantly affect the amount of asphaltenes in the support in the applied conditions.

With the pre-imbibition steps, the final asphaltene concentration in supports was 89 ± 12 mg/g, which is higher than experiments without this imbibition step but remains inside the acceptable repeatability. Thus, the pre-imbibition step does not significantly affect the amount of asphaltenes in the support in the applied conditions.

DOI: 10.1021/acs.energyfuels.5b01355
Energy Fuels 2015, 29, 6250−6258

The experiments at 1.8 and 9.0 MPa show the asphaltene concentrations in the support at 86 ± 12 and 81 ± 11 mg/g, respectively. These results were similar to the experiment at 5.0 MPa. Thus, it indicates that our asphaltene mass-transfer measurements was not affected by the pressure ranging from 1.8 to 9.0 MPa. *A fortiori*, the pressure evolution during the time stabilization at the beginning of the residence time does not significantly influence the results.

3.2. Different Residence Times. The diffusion of asphaltenes inside the porous media was monitored over time with experiments at 250 °C, about 5.0 MPa, and t_R ranging from 0 min (only the heating and cooling steps) to 3 weeks, to attempt to reach system equilibrium.

3.2.1. Mass Transfers in the System. The results of mass balances were summarized in Table 5.

The ratio of asphaltenes to support was adjusted to 360 ± 4 mg/g, with 724 ± 3 mg of initial asphaltenes introduced. The support mass increased from 60 mg with no residence time to up to nearly 400 mg after 3 weeks. On average, experiments had a mass balance of 97 ± 6 %, ensuring a fairly good confidence in the results.

The asphaltene concentrations on the supports were plotted as a function of the residence time in Figure 3. In the first few

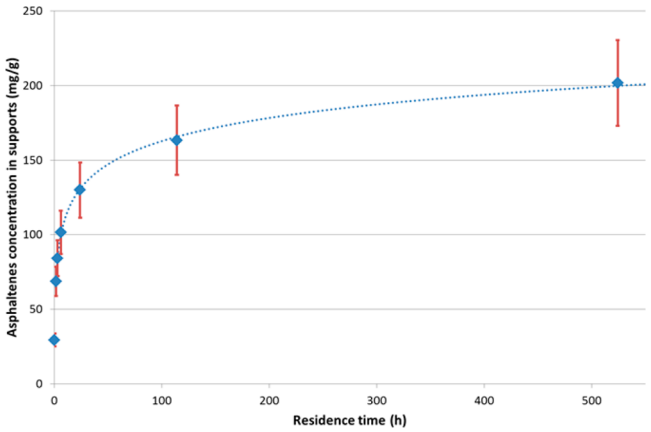

Figure 3. Evolution of the concentration of asphaltenes in the supports as a function of the residence time at 250 °C.

hours, 69 mg/g was adsorbed after 90 min, which corresponds to an initial penetration rate of 7.4×10^{-3} mg g^{-1} s^{-1}. In comparison, between 5 days and 3 weeks, the asphaltene penetration rate was 2.8×10^{-5} mg g^{-1} s^{-1}, which exhibits a decline of more than 99.5% of the initial penetration rate.

It can be noticed that after 3 weeks of exposure, there is still 43% of the total asphaltene amount in the supernatant.

3.2.2. Penetration Front in the Support. Optical microscopy observations of extrudates with several residence times were shown in Figure 4.

In the case of 0 min residence time, the center of extrudates is slightly colored. On the contrary, periphery presents a fine dark shell of 150 ± 10 μm of thickness. However, this core−shell repartition is modified as the residence time increases and seems no more distinguished after 6 h. Asphaltene penetration becomes much more pronounced and with gradual repartition. Above 24 h of residence time, extrudates are homogeneously black. Optical microscopy brings no sensitivity to discriminate samples beyond this point.

The alumina coloration is due to asphaltene penetration. However, because of the heterogeneous composition of

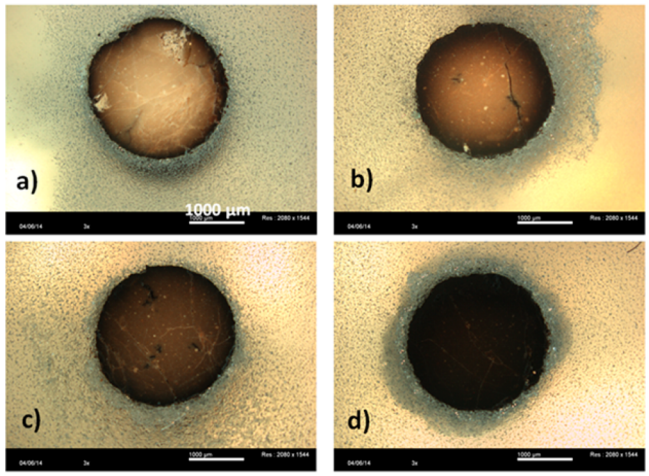

Figure 4. Optical microscopy images of supports exposed to asphaltene solutions at 250 °C for (a) 0 min, (b) 90 min, (c) 6 h, and (d) 24 h of residence time.

asphaltenes, no trivial links can be assessed between coloration and asphaltene concentration.

3.2.3. Porosity Changes. Porosity characterizations were summarized in Table 6. To compare support behavior, the porous volume and specific surface area were expressed in mL/g of alumina and m^2/g of alumina, respectively, using the calculated asphaltene concentrations from mass balance exploitation (Table 5). Pore distribution of the initial support and the extrudates from different residence time experiments were depicted in Figure 5.

It can be noticed that the specific surface area is experiencing small fluctuations in a scale of 25 m^2/g. However, several porosity parameters, such as pore diameter and porosity, change significantly through asphaltene deposition as well as pore diameter distribution.

The comparison between 0 min extrudates and the initial exhibits a decrease of the mean pore diameter from 14.5 to 12.8 nm during the heating and cooling steps. The pore volume was also depleted of 8% of the initial pore volume. It can be noticed that shapes of pore distribution are similar to the decline of large pores. This conservation of the shape of pore distribution indicates that asphaltenes reduce the pore volume in the whole pore size range, as if they covered the pore surface homogeneously.

When the residence time increases up to 1 day, a conservation of the distribution shape can also be seen. Asphaltene deposition has a stronger impact on porous volume reduction, as seen for 3 h extrudates in the pore diameter distribution. In the first day of exposure, the pore volume was depleted of 20% of the initial pore volume. From the initial support to 1 day of exposure, the range of large pores decreased by 2 nm, whereas the range of small pores remained fairly stable.

For the 1 day exposure point, it can be seen that, in addition of the decrease of pore volume, the distribution shape is expending to a smaller pore diameter. This tendency is confirmed for the 5 days and 3 weeks of exposure.

From 1 day to 3 weeks, the mean pore diameter is decreasing from 12.8 to 11.2 nm. After 3 weeks, the porous volume is depleted of 24% of the initial porous volume. It can be noticed that the majority of the pore volume cluttering is occurring during the first day of exposure. At this stage, the decrease of

DOI: 10.1021/acs.energyfuels.5b01355
Energy Fuels 2015, 29, 6250−6258

Table 6. Porosity Characteristics of the Supports after Diffusion Experiments

	0 min	90 min	3 h	1 day	5 days	3 weeks
specific surface area, S_{BET} ($m^2/g_{alumina}$)	186 ± 10	182 ± 10	179 ± 10	183 ± 10	172 ± 10	196 ± 10
parameter C from the BET	102 ± 5	84 ± 4	79 ± 4	61 ± 3	54 ± 3	48 ± 2
porous volume, V_{BJH} ($mL/g_{alumina}$)	0.73 ± 0.04	0.71 ± 0.04	0.68 ± 0.03	0.64 ± 0.03	0.59 ± 0.03	0.61 ± 0.03
mean pore diameter, d_{mean} (nm)	12.8 ± 0.6	12.6 ± 0.6	12.7 ± 0.6	12.8 ± 0.6	11.5 ± 0.6	11.2 ± 0.6
structural density, ρ_{struc} (mL/g)	2.98 ± 0.30	2.97 ± 0.30	2.79 ± 0.28	2.54 ± 0.25	2.53 ± 0.25	2.49 ± 0.25
porosity, ε (%)	68 ± 3	66 ± 3	65 ± 3	58 ± 3	59 ± 3	55 ± 3

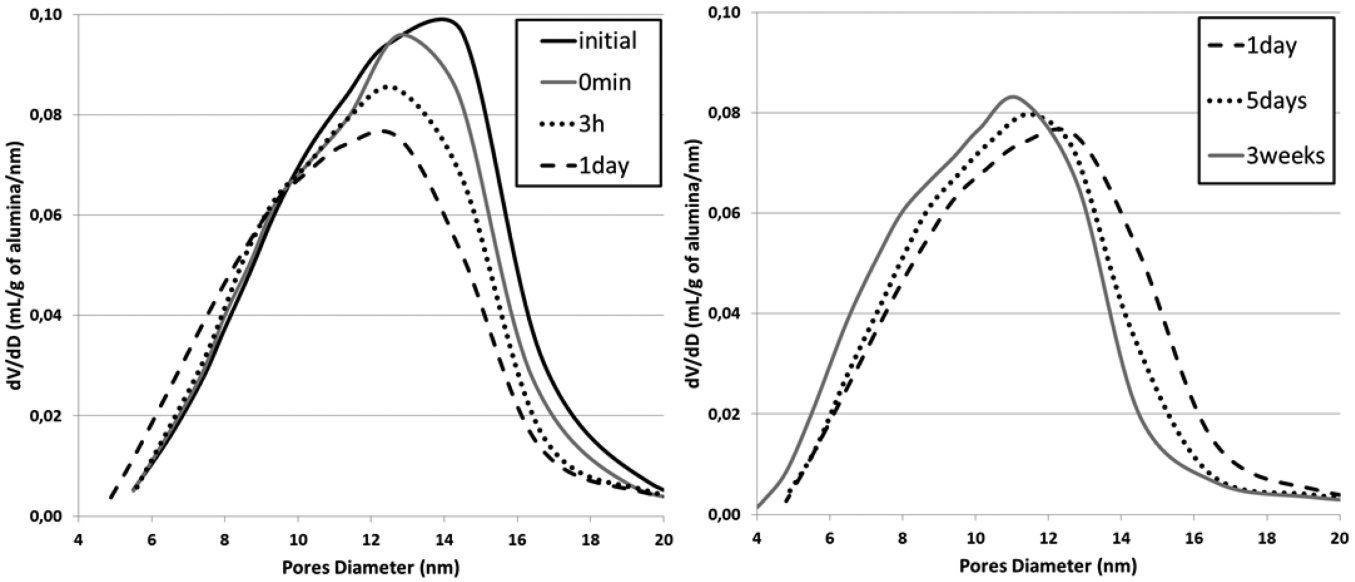

Figure 5. Pore diameter distribution by nitrogen desorption analysis over residence time.

the pore volume slows and turns to stagnate. However, the specific surface increased from 5 days to 3 weeks, which can indicate that the asphaltene deposition creates a surface. In parallel, the population of smaller pores is increasing. It translates to a second stage of the pore network cluttering phenomenon with pore network occlusion.

To highlight differences in asphaltene deposition on alumina, the parameters C from the BET method were plotted as a function of the asphaltene concentration in supports in Figure 6.

This figure shows a linear evolution of the parameter C with the asphaltene concentration in supports until a concentration of 130 mg/g (extrudates after 1 day of exposure). For higher concentrations, the parameter C is less impacted by the asphaltene adsorption.

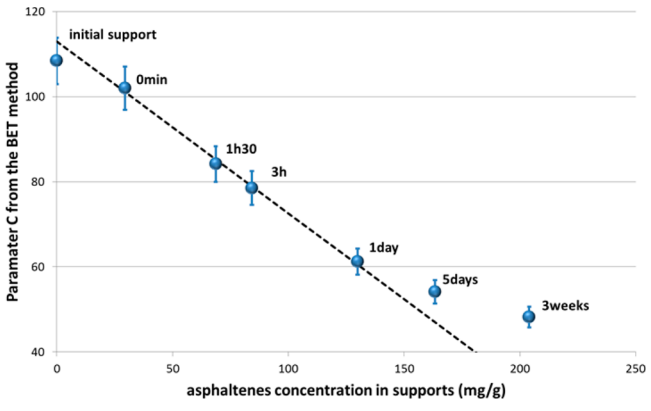

Figure 6. Parameters C from the BET method as a function of the asphaltene concentration in supports.

The parameter C is a rough guide to the magnitude of nitrogen affinity to the support surface.[28] The evolution of C indicates that the asphaltene deposition affected the pore surface from a 1 day exposure point differently, which is in accordance with our previous observations on the pore size distributions (cf. to Figure 5). The change of the C tendency can be interpreted as a consequence of several phenomena, such as a different arrangement of asphaltene deposition or the pore network plugging.

To highlight potential occluded volume with the asphaltene deposition, the experimental structural density and porosity were compared to a theoretical case of homogeneous deposition without occluded volume.

In the case of non-occluded volume, the theoretical structural density of an impregnated support can be expressed as a function of its asphaltene content. Consider the mass, m_i, and the volume, V_i, of an impregnated support with the following equations:

$$m_i = m_{al}(1 + X_i) \tag{6}$$

$$V_i = m_{al}\left(\frac{1}{\rho_{al}} + \frac{X_i}{\rho_{asp}}\right) \tag{7}$$

with m_{al} being the mass of alumina in grams, ρ_{al} being the structural density of the initial alumina support in g/mL, ρ_{asp} being the structural density of the asphaltenes in g/mL, and X_i being the asphaltene content of the impregnated support in grams of asphaltenes per gram of alumina

DOI: 10.1021/acs.energyfuels.5b01355
Energy Fuels 2015, 29, 6250−6258

The structural density of the impregnated support, $\rho_i = m_i/V_i$, becomes

$$\rho_i = \frac{1 + X_i}{\frac{1}{\rho_{al}} + \frac{X_i}{\rho_{asp}}} \quad (8)$$

To calculate the theoretical porosity, ε_i, as a function of the asphaltene content, the porosity was considered as follows:

$$\varepsilon_i = \frac{V_{ex} - V_{al} - V_{asp}}{V_{ex}} \quad (9)$$

with V_{ex} being the volume of an extrudate, V_{al} being the volume of alumina present in the extrudate, and V_{asp} being the volume of asphaltenes in the extrudate.

With the assumption that the volume of an extrudate is constant through asphaltene deposition, the volume of alumina can be expressed with the initial porosity of the support, ε_{al}.

$$V_{al} = V_{ex}(1 - \varepsilon_{al}) \quad (10)$$

The volume of asphaltenes adsorbed can be expressed with this volume, the asphaltene content, and the structural density of asphaltenes, ρ_{asp}, and alumina, ρ_{al}.

$$V_{asp} = \frac{V_{al}\rho_{al}X_i}{\rho_{asp}} \quad (11)$$

Therefore, the theoretical porosity, ε_i, for an impregnated support with a homogeneous asphaltene deposition becomes a function of the asphaltene content of the support.

$$\varepsilon_i = \varepsilon_{al} - \frac{(1 - \varepsilon_{al})\rho_{al}X_i}{\rho_{asp}} \quad (12)$$

The structural density of the initial alumina support, ρ_{al}, and the initial porosity, ε_{al}, were measured at 3.22 ± 0.32 g/mL and 71 ± 4%, respectively (cf. Table 2). The structural density of dried initial asphaltenes, ρ_{asph}, was also measured with mercury porosimetry at 1.22 ± 0.12 g/mL (cf. Table 1). This measurement is consistent with the asphaltene density reported in the literature at 1.2 g/mL.[29−31] From these measurements, the theoretical density and porosity were plotted in parallel of experimental measurements in Figure 7.

The structural density and the porosity tendency are consistent with a homogeneous asphaltene deposition phenomenon, even during the second stage of deposition observed in the pore diameter distribution (cf. to Figure 5) and the parameter C (cf. to Figure 6). After 3 weeks of exposure, the support porosity characterizations show no evidence of pore plugging as a result of asphaltene deposition. The analytical techniques have not been able to detect the blockage of pore network connectivity.

3.2.4. Asphaltene Adsorption Model. During our experiment, believing the porosity and structural density tendency, significant plugging in the pore network was not detected. However, two stages of deposition can be clearly seen in pore distribution progression; asphaltene penetration becomes much more pronounced and with gradual repartition.

In the first day of exposure, the asphaltene penetration front is gradual in the extrudates as a result of a slow diffusion. The pore network cluttering is occurring homogeneously with the decrease of the mean pore diameter and pore volume conserving the same size distribution shape. The range of large pores is also reduced, whereas the range of small pores

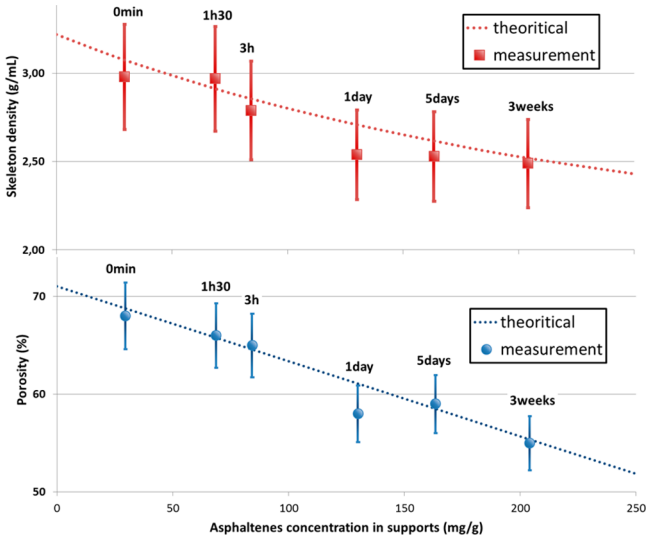

Figure 7. Structural density and porosity as a function of the asphaltene concentration.

remained stable. The pore surface seems to be homogeneously covered by asphaltenes.

When the exposure time increased to several days until 3 weeks, a second mode of asphaltene deposition is occurring. From the pore size distribution, the increase of the number of small mesopores is occurring, which is changing the distribution of the pore diameter and has less impact in the porous volume decrease but increases the specific surface area.

We propose an asphaltene pore cluttering model to explain this phenomenon (see Figure 8). In the first step of asphaltene adsorption, the aggregates will homogeneously cover the pore surface. This first phenomenon leads to a decrease of the mean pore diameter and does not affect the shape of pore size distribution. The large pores are progressively reduced. However, when a pore reaches a small size, it will reduce the affinity of asphaltenes for their deposition to pore blockage. It will induce changes in the global pore distribution with the growth of this kind of small pores and the creation of a specific surface by asphaltene deposition.

We can compare this asphaltene adsorption behavior on the porous network to the coke deposit often observed during industrial processes. Previous works have shown that pore plugging can occur during the aging of the catalyst by coke deposition.[32] It seems not to be the case for asphaltene diffusion, even at a high temperature, suggesting a slow and hindered diffusion mechanism through the porosity and, finally, an adsorption of the molecule on the alumina surface. However, in the case of reaction and conversion of asphaltenes, the formation of lighter compounds might influence the proposed model and boost the diffusion of these lighter compounds. The presence of a catalyst with active sites will also probably enhance the adsorption of asphaltenes on an alumina surface.

4. CONCLUSION

For the first time, the asphaltene diffusion and adsorption into porous media at a high temperature and pressure were monitored and characterized in terms of the mass transfer, penetration depth, and porosity cluttering.

Our procedure was successfully tested in terms of limits of detection and quantification. Blank testing gave good

DOI: 10.1021/acs.energyfuels.5b01355
Energy Fuels 2015, 29, 6250−6258

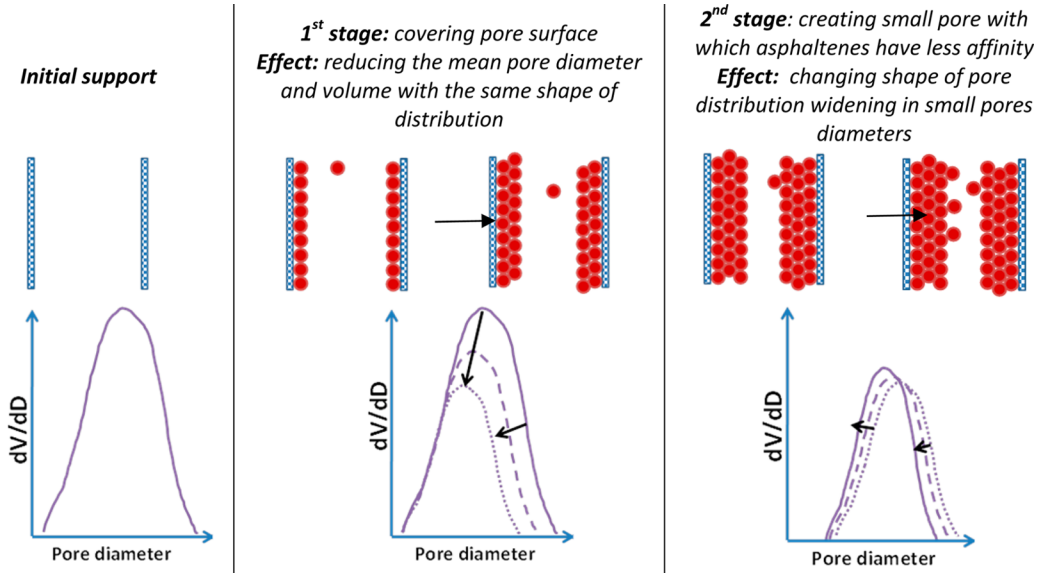

Figure 8. Summary of the asphaltene deposition model.

confidence in our results as well as repeatability tests. Moreover, several parameters, such as stirring, imbibition, and pressure, showed no significantly impact on asphaltene diffusion measurements in the investigated range of experimental parameters.

Under the studied temperature and pressure, the asphaltene mass-transfer process remained slow, with several weeks being needed to reach system equilibrium. No pore plugging was detected through the porosity exploitation. However, the change in the pore network distribution allows us to propose an asphaltene pore cluttering model to explain the two-stage phenomenon. This model is constituted of two subsequent steps depending upon the pore size. The pore surface is homogeneously covered in the first step until pore diameter reaches the size of asphaltene aggregates. In the second step, the asphaltenes have less affinity with this kind of pore, which lead to the growth of their number.

AUTHOR INFORMATION

Corresponding Author

*Telephone: +33-4-37-70-29-43. E-mail: didier.espinat@ifpen.fr.

Notes

The authors declare no competing financial interest.

ACKNOWLEDGMENTS

The Laboratory of Textural and Mechanical Characterization of IFPEn is thanked for their help and expertise on the porosity characterization of various supports to achieve this work. The financial support of IFPEn for funding this study is greatly acknowledged.

REFERENCES

(1) Leon, O.; Rogel, E. J.; Espidel, J.; Torres, G. A. *Energy Fuels* **2000**, *14*, 6−10.
(2) Rogel, E. J. *Energy Fuels* **2000**, *14*, 566−574.
(3) Bartholdy, J.; Andersen, S. I. *Energy Fuels* **2000**, *14*, 52−55.
(4) Merdrignac, I.; Espinat, D. *Oil Gas Sci. Technol.* **2007**, *62*, 7−32.
(5) Espinat, D.; Fenistein, D.; Barré, L.; Frot, D.; Briolant, Y. *Energy Fuels* **2004**, *18*, 1243−1249.
(6) Durand, E.; Clemancey, M.; Lancelin, J. M.; Verstraete, J.; Espinat, D.; Quoineaud, A. A. *Energy Fuels* **2010**, *24*, 1051−1062.
(7) Eyssautier, J.; Hénaut, I.; Levitz, P.; Espinat, D.; Barré, L. *Energy Fuels* **2012**, *26*, 2696−2704.
(8) da Silva Oliveira, E. C.; Neto, A. C.; Lacerda, V., Jr.; de Castro, E. V. R.; de Menezes, S. M. C. *Fuel* **2014**, *117*, 146−151.
(9) Mullins, O. C.; Sabbah, H.; Eyssautier, J.; Pomerantz, A. E.; Barre, L.; Andrews, A. B.; Ruiz-Morales, Y.; Mostowfi, F.; McFarlane, R.; Goual, L.; Lepkowicz, R.; Cooper, T.; Orbulescu, J.; Leblanc, R. M.; Edwards, J.; Zare, R. N. *Energy Fuels* **2012**, *26*, 3986−4003.
(10) Andrews, A. B.; Shih, W. C.; Mullins, O. C.; Norinaga, K. *Appl. Spectrosc.* **2011**, *65*, 1348−1356.
(11) Yudin, I. K.; Anisimov, M. A. Dynamic light scaterring monitoring of asphaltene aggregation in crude oils and hydrocarbon solutions. *Asphaltenes, Heavy Oils, and Petroleomics*; Springer: New York, 2007; Vol. *17*, p 439.
(12) Durand, E.; Clemancey, M.; Lancelin, J. M.; Verstraete, J.; Espinat, D.; Quoineaud, A. A. *J. Phys. Chem. C* **2009**, *113*, 16266−16276.
(13) Durand, E. Extrapolation of NMR techniques from biology to the study of heavy oil compounds. Ph.D. Dissertation, University Lyon 1, Lyon, France, 2009.
(14) Baltus, R. E.; Anderson, J. L. *Chem. Eng. Sci.* **1983**, *38*, 1959−1969.
(15) Marchal, C.; Abdessalem, E.; Tayakout-Fayolle, M.; Uzio, D. *Energy Fuels* **2010**, *24*, 4290−4300.
(16) Roussi, L.; Stihle, J.; Geantet, C.; Uzio, D.; Tayakout-Fayolle, M. *Fuel* **2013**, *109*, 167−177.
(17) Tayakout, M.; Ferreira, C.; Espinat, D.; Picon, S. A.; Sorbier, L.; Guillaume, D.; Guibard, I. *Chem. Eng. Sci.* **2010**, *65*, 1571−1583.
(18) Meirer, F.; Kalirai, S.; Morris, D.; Soparawalla, S.; Liu, Y.; Mesu, G.; Andrews, J. C.; Weckhuysen, B. M. *Science Advances* **2015**, *1* (3), e1400199.
(19) Wang, G.; Chen, Z. T.; Lan, X. Y.; Wang, W.; Xu, C. M.; Gao, J. S. *Chem. Eng. Sci.* **2011**, *66*, 1200−1211.
(20) Marques, J.; Baudot, A.; Merdrignac, I.; Guillaume, D.; Espinat, D.; Brunet, S. *Proceedings of the 235th ACS National Meeting*; New Orleans, LA, April 6−10, 2008; 99010.
(21) Barbier, J.; Marques, J.; Caumette, G.; Merdrignac, I.; Bouyssiere, B.; Lobinski, R.; Lienemann, C. P. *Fuel Process. Technol.* **2014**, *119*, 185−189.
(22) Rainer, D. R.; Rautiainen, E.; Imhof, P. *Appl. Catal., A* **2003**, *249*, 69−80.
(23) Brunauer, S.; Emmett, P. H.; Teller, E. *J. Am. Chem. Soc.* **1938**, *60*, 309−319.

DOI: 10.1021/acs.energyfuels.5b01355
Energy Fuels 2015, 29, 6250−6258

(24) Rouquerol, F.; Rouquerol, J.; Sing, K. S. W.; Llewellyn, P.; Maurin, G. *Adsorption by Powders and Porous Solids*, 2nd ed.; Academic Press: Waltham, MA, 2013.
(25) Allen, T. *Particle Size Measurement*, 3rd ed.; Springer: New York, 1981; Powder Technology Series.
(26) Barrett, E. P.; Joyner, L. G.; Halenda, P. P. *J. Am. Chem. Soc.* **1951**, *73*, 373−380.
(27) Le Page, J. F.; Chatila, S. G.; Davidson, M. *Raffinage e Conversion des Produits Lourds du Pétrole*; Technip: Paris, France, 1990.
(28) Gregg, S. J.; Sing, K. S. W. *Adsorption, Surface Area and Porosity*; Academic Press: Waltham, MA, 1967.
(29) Mullins, O. C.; Sheu, E. Y.; Hammami, A.; Marshall, A. G. *Asphaltenes, Heavy Oils, and Petroleomics*; Springer: New York, 2007.
(30) Savvidis, T. G.; Fenistein, D.; Barre, L.; Behar, E. *AIChE J.* **2001**, *47*, 206−211.
(31) Roux, J. D.; Broseta, D.; Demé, B. *Langmuir* **2001**, *17*, 5085−5092.
(32) Espinat, D.; Freund, E.; Dexpert, H.; Martino, G. *J. Catal.* **1990**, *126*, 496−518.

DOI: 10.1021/acs.energyfuels.5b01355
Energy Fuels 2015, 29, 6250−6258